Small–Signal Analysis of Open–Loop PWM Flyback DC–DC Converter for CCM

Marian K. Kazimierczuk, Senior Member, IEEE, and Sonny T. Nguyen
Wright State University
Department of Electrical Engineering
Dayton, OH 45435, U. S. A.
Phone: (513)873–5059 and FAX: (513)873–5009

Abstract— **A flyback dc–dc converter is obtained from the conventional buck–boost converter by replacing the inductor with an isolation transformer. A transformer in the flyback converter is used to achieve a dc isolation between the input and the output of the converter. This paper presents dc and small–signal circuit models for the flyback converter for continuous conduction mode (CCM). The parasitic components are included in these models. The dc model is used to derive the equations for the dc voltage transfer function and the efficiency. The small–signal model is used to derive the equations for the open–loop small–signal transfer functions, such as control–to–output transfer function, input–to–output transfer function, input impedance, and output impedance. Bode plots are also given for the small–signal transfer functions.**

I. Introduction

The PWM flyback dc–dc converter is a transformer version of the buck–boost converter. The transformer provides a dc insulation between the input and output of the converter. The transformer also allows the converters to achieve much higher or lower values of the dc voltage transfer function than its transformerless counterpart. The operating frequency of PWM flyback converter can be on the order of 100 kHz. Therefore, a high-frequency transformer is used, which is much smaller and lighter than low-frequency transformers operating at 50 or 60 Hz. The purpose of this paper is to introduce a simple method of obtaining dc and small–signal circuit models of PWM flyback dc–dc converter for CCM and derive open–loop transfer functions.

II. Converter Description

Fig. 1 shows a basic circuit of the PWM flyback dc–dc power converter. It is comprised of a controllable switch S such as a power MOSFET (other power switches such as a BJT, a IGBT, or an MCT can also be used), a diode D_2, a filter capacitor C, a load resistance R, and an isolation transformer. A transformer is used to achieve a dc isolation. The voltage across the coils of the transformer is directly proportional to the number of turns of the coils and the current in the coils of the transformer is inversely proportional to the number of turns. Therefore, the relationship is expressed by the formula

$$\frac{v_p}{v_{sec}} = \frac{N_p}{N_{sec}} = \frac{i_{sec}}{i_p} = n \qquad (1)$$

where

v_p = voltage on the primary side, V
v_{sec} = voltage on the secondary side, V
N_p = number of turns of the primary winding

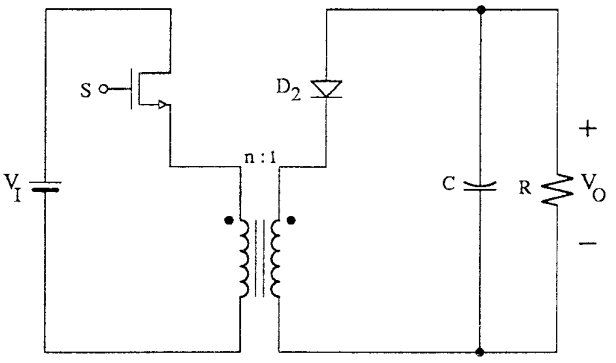

Fig. 1: Basic circuit of the PWM flyback dc–dc power converter.

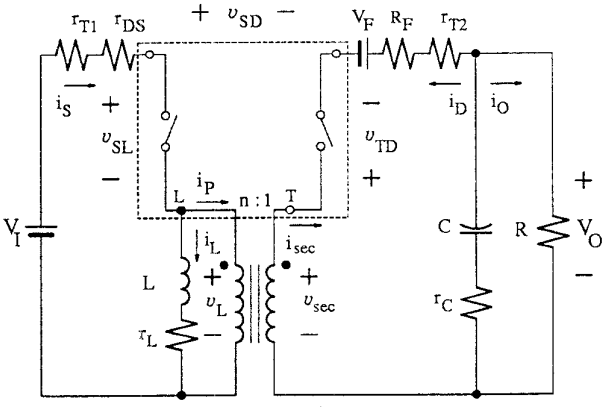

Fig. 2: Equivalent circuit of the PWM flyback converter with actual components.

N_{sec} = number of turns of the secondary winding
i_p = current in the primary side, A
i_{sec} = current in the secondary side, A.

The isolation transformer turns ratio n:1 is chosen to give a suitable switch duty ratio D for a given output voltage V_O and line input voltage V_I.

The switch S is turned ON and OFF by a driver at the switching frequency $f_s = 1/T$ with the ON duty ratio $D = t_{on}/T$, where t_{on} is the interval when the switch is ON. Fig. 2 depicts an equivalent circuit of the converter, where r_{DS} is the transistor ON–resistance, r_{T1} is the winding resistance of the primary side of the transformer and is

CH35797–95/0000–0069 $1.00©1995 IEEE

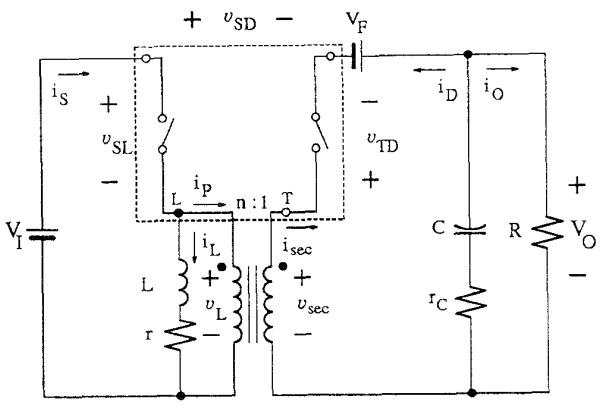

Fig. 3: An equivalent circuit with an EAR r connected in series with the magnetizing inductance L.

connected in series with r_{DS}, r_{T2} is the winding resistance of the secondary side of the transformer and is connected in series with R_F, r_L is the dc ESR of the inductor, V_F is the threshold voltage of the diode, R_F is the forward resistance of the diode, and r_C is the ESR of the filter capacitor. Fig. 3 shows the equivalent circuit of the converter with the equivalent averaged resistance (EAR) r connected in series with the magnetizing inductance L.

III. Assumptions

The analysis of PWM flyback converter of Fig. 1 begins with the following assumptions:

1) The power MOSFET in the ON state is modeled by a constant resistance r_{DS} and in the OFF state by an infinite resistance. Its output capacitance and lead inductance (and thereby switching losses) are zero.

2) The diode in the ON state is modeled by a constant-voltage battery V_F and a forward resistance R_F and in the OFF state by an infinite resistance. The charge-carrier lifetime is zero for p–n junction diode (and therefore switching losses due to the reverse recovery are zero), the diode junction capacitance and lead inductance are zero.

3) Passive components are linear, time-invariant, and frequency-independent.

4) The output impedance of the input voltage source is zero for both dc and ac components.

5) The frequencies of ac components of the input voltage and the duty cycle are lower than one-half the switching frequency, similarly as for the state-space averaging method [2], [3].

6) The transformer leakage inductances and the stray capacitances are neglected.

IV. Equivalent Averaged Resistance

The EAR of the parasitic resistances is found using *the principle of energy conservation method.* The inductor current i_L for ON interval $0 < t \leq DT$ and OFF interval $DT < t \leq T$ is given by

$$i_L = \begin{cases} \frac{\Delta i_L}{DT} t + I_L - \frac{\Delta i_L}{2}, & \text{for } 0 < t \leq DT \\ -\frac{\Delta i_L}{(1-D)T}(t - DT) + I_L + \frac{\Delta i_L}{2}, & \text{for } DT < t \leq T. \end{cases} \tag{2}$$

Letting

$$i_{L1} = \frac{\Delta i_L}{DT} t + I_L - \frac{\Delta i_L}{2} \tag{3}$$

$$i_{L2} = -\frac{\Delta i_L}{(1-D)T}(t - DT) + I_L + \frac{\Delta i_L}{2} \tag{4}$$

the rms value of inductor current I_{Lrms} is

$$I_{Lrms}^2 = \frac{1}{T}\int_0^{DT} i_{L1}^2 dt + \frac{1}{T}\int_{DT}^{T} i_{L2}^2 dt = I_L^2 D(1 + k_I^2)$$

$$= \frac{I_D^2}{n^2(1-D)^2}(1 + k_I^2) = \frac{I_S^2}{D^2}(1 + k_I^2) \tag{5}$$

where

$$k_I = \frac{n^2 R(1-D)^2}{\sqrt{12} f_s L}. \tag{6}$$

The power loss in r_L is

$$P_{rL} = r_L I_{Lrms}^2 = r_L I_L^2 (1 + k_I^2). \tag{7}$$

The EAR of the r_L in the inductor branch is

$$r_{L(EAR)} = r_L(1 + k_I^2). \tag{8}$$

The switch current at the ON interval $0 < t \leq DT$ and OFF interval $DT < t \leq T$ is given by

$$i_S = \begin{cases} \frac{\Delta i_L}{DT} t + I_L - \frac{\Delta i_L}{2}, & \text{for } 0 < t \leq DT \\ 0, & \text{for } DT < t \leq T. \end{cases} \tag{9}$$

The rms value of the switch current I_{Srms} is

$$I_{Srms}^2 = \frac{1}{T}\int_0^{DT} i_S^2 dt$$

$$= I_L^2 D(1 + k_I^2) = I_S^2 \frac{(1 + k_I^2)}{D} = \frac{I_D^2(1 + k_I^2)}{n^2(1-D)^2}. \tag{10}$$

The power dissipated in the resistance r_{DS} is

$$P_{rDS} = r_{DS} I_{Srms}^2 = r_{DS} I_L^2 D(1 + k_I^2)$$

$$= \frac{r_{DS} I^2(1 + k_I^2)}{D} = \frac{I_D^2 D(1 + k_I^2)}{n^2(1-D)^2}. \tag{11}$$

Since $P_{rDS(EAR)} = P_{rDS}$ and $P_{rDS(EAR)} = r_{DS(EAR)} I_L^2$, the EAR of the ON-resistance r_{DS} in the inductor branch is

$$r_{DS(EAR)} = r_{DS} D(1 + k_I^2). \tag{12}$$

Similarly, the EAR of r_{T1} is

$$r_{T1(EAR)} = r_{T1} D(1 + k_I^2). \tag{13}$$

The diode current for ON interval $0 < t \leq DT$ and OFF $DT < t \leq T$ is given by

$$i_D = \begin{cases} 0, & \text{for } 0 < t \leq DT \\ n\left[-\frac{\Delta i_L}{(1-D)T}(t - DT) + I_L + \frac{\Delta i_L}{2}\right], & \text{for } DT < t \leq T. \end{cases} \tag{14}$$

The rms value of the diode current I_{Drms} is

$$I_{Drms}^2 = \frac{1}{T}\int_{DT}^{T} i_D^2 dt = n^2 I_L^2(1-D)(1+k_I^2)$$

$$= \frac{I_S^2 n^2(1-D)(1+k_I^2)}{D^2} = \frac{I_D^2(1+k_I^2)}{(1-D)}. \quad (15)$$

The power loss in R_F is

$$P_{RF} = R_F I_{Drms}^2 = R_F I_L^2 n^2(1-D)(1+k_I^2). \quad (16)$$

Since the power dissipated $P_{RF(EAR)} = R_F I_L^2$ is equal to power loss P_{RF}, the EAR of the diode forward resistance R_F in the inductor branch is

$$R_{F(EAR)} = R_F n^2(1-D)(1+k_I^2). \quad (17)$$

Similarly, the EAR of r_{T2} is

$$r_{T2(EAR)} = r_{T2} n^2(1-D)(1+k_I^2). \quad (18)$$

Because the voltage across the filter capacitor is constant during the time interval $(1-D)T$, the average inductance current I_L flows through the parallel combination of r_C and R during the time interval DT, resulting in the resistance connected in series with the diode

$$r_{RC} = \frac{D}{1-D}(r_C||R) = \frac{D}{1-D}\frac{Rr_C}{R+r_C}. \quad (19)$$

Hence, the EAR of r_{RC} is

$$r_{RC(EAR)} = n^2(1-D)^2 r_{RC}. \quad (20)$$

Finally, all the EAR is

$$r = r_{L(EAR)} + r_{DS(EAR)} + r_{T1(EAR)} + R_{F(EAR)}$$
$$+ r_{T2(EAR)} + r_{RC(EAR}$$
$$= [r_L + (r_{DS} + r_{T1})D + n^2(R_F + r_{T2})(1-D)] \times$$
$$(1+k_I^2) + n^2 D(1-D)\frac{Rr_C}{R+r_C}. \quad (21)$$

Note that the value of k_I is very small and therefore, it can be neglected.

The *dc voltage transfer function* of the idealized switching part (*the input-to-output voltage conversion ratio*) is

$$M_{VDC} = \frac{V_O}{V_I} = \frac{I_I}{I_O} = -\frac{D}{n(1-D)}. \quad (22)$$

V. DC AND AC MODELS FOR THE IDEAL SWITCHING PART

The voltage across diode D_2 during the ON interval $0 < t \leq DT$ is

$$v_D = \frac{V_I}{n} - V_O = \frac{V_I}{n} + |V_O|. \quad (23)$$

Hence, the average voltage across the diode can be found as

$$V_{TD} = \frac{1}{T}\int_0^{DT}\left(\frac{V_I}{n} - V_O\right) = D\left(\frac{V_I}{n} - V_O\right)$$

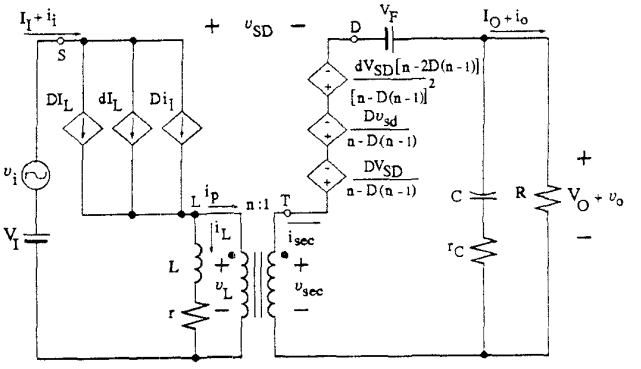

Fig. 4: Circuit model of the PWM flyback converter for the dc and small-signal components.

$$= D\left(\frac{V_O}{nM_{VDC}} - V_O\right) = D\left[-\frac{(1-D)V_O}{D} - V_O\right] = -V_O. \quad (24)$$

Since $v_{SD} = V_I - V_O$, the average value of this voltage is

$$V_{SD} = V_I - V_O = \frac{V_O}{M_{VDC}} - V_O = -V_O\left[\frac{n(1-D)+D}{D}\right]$$

$$= V_{TD}\left[\frac{n(1-D)+D}{D}\right]. \quad (25)$$

Thus,

$$V_{TD} = \frac{D}{n(1-D)+D}V_{SD} = \frac{DV_{SD}}{n-D(n-1)}. \quad (26)$$

Because $i_S \approx I_L$ for $0 < t \leq DT$, the average switch current is

$$I_S = \frac{1}{T}\int_0^{DT} i_S dt = DI_L. \quad (27)$$

The total instantaneous quantities of the flyback converter can be expressed as the sums of the dc and ac components

$$i_S = I_S + i_s \quad (28)$$

$$i_L = I_L + i_l \quad (29)$$

$$i_D = I_D + i_d \quad (30)$$

$$v_S = V_S + v_s \quad (31)$$

$$d_T = D + d \quad (32)$$

$$v_{SD} = V_{SD} + v_{sd} \quad (33)$$

$$v_{TD} = V_{TD} + v_{td} \quad (34)$$

$$v_I = V_I + v_i \quad (35)$$

$$v_O = V_O + v_o. \quad (36)$$

From (27) and (26),

$$i_S = d_T i_L \quad (37)$$

and

$$v_{TD}[n - d_T(n-1)] = d_T v_{SD}. \quad (38)$$

Substitution of (28) and (32) into (36) yields

$$i_S = I_S + i_s = (D+d)(I_L + i_l) = DI_L + Di_l + I_L d + di_l. \quad (39)$$

Substitution of (32), (33), and (34) into (38), one obtains

$$(V_{TD} + v_{td})[n - (D+d)(n-1)] = (D+d)(V_{SD} + v_{sd})$$

$$V_{TD}[n - D(n-1)] + V_{TD} d(n-1) + v_{td}[n - D(n-1)] + v_{td} d(n-1)$$
$$= DV_{SD} + DV_{SD} + dV_{SD} + dv_{sd}. \quad (40)$$

Hence,

$$V_{TD} + v_{td} = \frac{DV_{SD}}{n - D(n-1)} + \frac{Dv_{sd}}{n - D(n-1)} +$$
$$\frac{d[V_{SD} - V_{TD}(n-1)]}{n - D(n-1)} + \frac{d[v_{sd} - v_{td}(n-1)]}{n - D(n-1)}. \quad (41)$$

Substitution of equation (26) into (41) yields

$$V_{TD} + v_{td} = \frac{DV_{SD}}{n - D(n-1)} + \frac{v_{sd} D}{n - D(n-1)} +$$
$$\frac{dV_{SD}}{n - D(n-1)} \left[1 - \frac{D(n-1)}{n - D(n-1)}\right] + \frac{d[v_{sd} - v_{td}(n-1)]}{n - D(n-1)}$$
$$= \frac{DV_{SD}}{n - D(n-1)} + \frac{Dv_{sd}}{n - D(n-1)} +$$
$$\frac{dV_{SD}[n - 2D(n-1)]}{[n - D(n-1)]^2} + \frac{d[v_{sd} - v_{td}(n-1)]}{n - D(n-1)}. \quad (42)$$

Since the magnitudes of the ac components are assumed to be much lower than the dc components, a linear circuit model of flyback converter for the dc and small-signal operation can be obtained by neglecting the current dependent source di_l and voltage dependent source $d[v_{sd} - v_{td}(n-1)]/[n - D(n-1)]$ in (39) and (42). Equations (39) and (42) can be represented by current and voltage sources of the flyback converter as shown in Fig. 4. Now, the principle of superposition can be used to derive the dc shown in Fig. 5 and small-signal model shown in Fig. 6.

VI. DC Characteristics

From the dc model shown in Fig. 5, the *dc input-to-output voltage transfer function* (also called the *dc voltage gain*) can be expressed as

$$M_{VDC} \equiv \frac{V_O}{V_I} = -\frac{D}{n(1-D)} \frac{1}{\left[1 - \frac{V_F}{V_O} + \frac{[n - D(n-1)]r}{n(1-D)^2 R}\right]}. \quad (43)$$

The *efficiency* of the flyback converter is

$$\eta \equiv \frac{V_O I_O}{V_I I_I} = M_{VDC} M_{IDC} = \frac{1}{1 - \frac{V_F}{V_O} + \frac{[n - D(n-1)]r}{n(1-D)^2 R}} \quad (44)$$

where

$$M_{IDC} = -\frac{n(1-D)}{D} \quad (45)$$

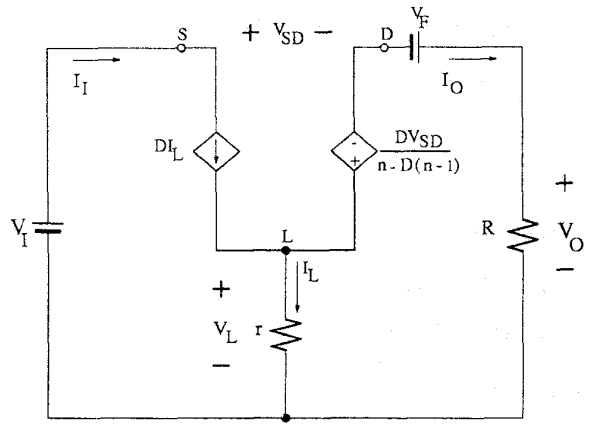

Fig. 5: Dc model of the PWM flyback converter.

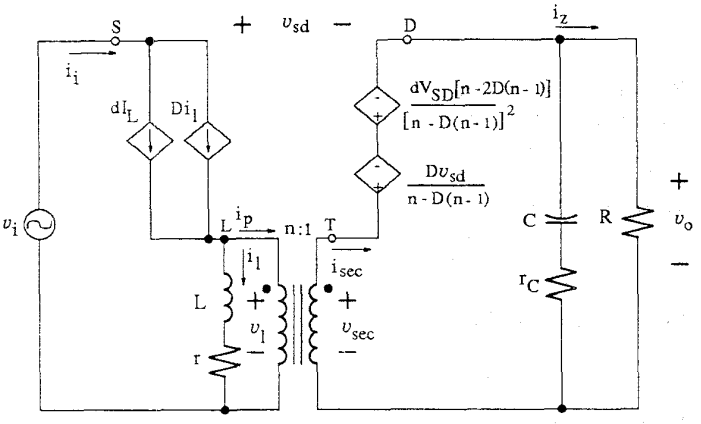

Fig. 6: Small-signal model of the PWM flyback converter.

and $V_O < 0$ and $I_O < 0$.

Figs. 7 and 8 show the plots of the magnitude of dc gain characteristics $|M_{VDC}|$ and the efficiency of the converter η as functions of D for different values of $R = 14$ (solid line), 28, and 140 Ω, $V_O = 28$ V, $r_L = 1.7$ Ω, $r_{DS} = 0.5$ Ω, $V_F = 0.7$ V, turn ratio = 5, $r_{T1} = 20$ mΩ, $r_{T2} = 10$ mΩ, and $R_F = 25$ mΩ. These parameters are for the flyback converter, which is designed in the Appendix.

VII. Small-Signal Characteristics

The small-signal dynamic characteristics of PWM flyback converter can be derived using the small-signal model which is shown in Fig. 6.

A. Control-to-Output Voltage Transfer Function

The control-to-output (or *duty ratio-to-output*) voltage transfer function in the frequency domain is found as

$$T_p(s) \equiv \frac{v_o(s)}{d(s)}\Big|_{v_i(s)=0}$$

$$= -\frac{nV_O r_C}{(1-D)(R + r_C)} \frac{(s - z_n)(s - z_p)}{s^2 + 2\xi\omega_0 s + \omega_0^2}$$

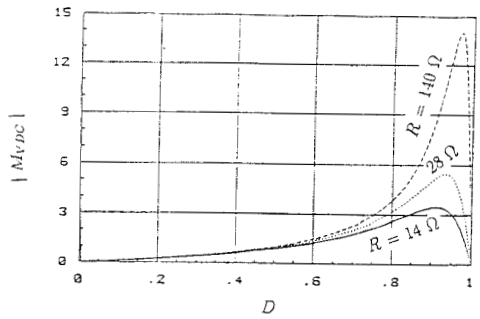

Fig. 7: Plot of $\mid M_{VDC} \mid$ as a function of D.

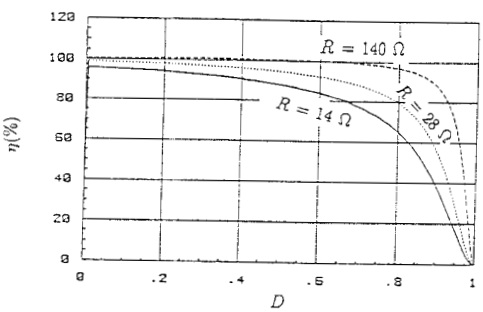

Fig. 8: Plot of converter efficiency η as a function of D.

$$= -\frac{nV_O r_C z_n z_p}{(1-D)(R+r_C)\omega_0^2} \frac{\left(1-\frac{s}{z_n}\right)\left(1-\frac{s}{z_p}\right)}{1+\frac{s}{\omega_0 Q}+\frac{s^2}{\omega_0^2}}$$

$$= -\frac{nV_O r_C}{(1-D)(R+r_C)} \frac{(s+\omega_{zn})(s-\omega_{zp})}{s^2+2\xi\omega_0 s+\omega_0^2}$$

$$= -\frac{nV_O r_C \omega_{zn}\omega_{zp}}{(1-D)(R+r_C)\omega_0^2} \frac{\left(1+\frac{s}{\omega_{zn}}\right)\left(1-\frac{s}{\omega_{zp}}\right)}{1+\frac{s}{\omega_0 Q}+\frac{s^2}{\omega_0^2}}. \quad (46)$$

The frequency of the negative (LHP) zero is

$$\omega_{zn} = -z_n = \frac{1}{Cr_C}. \quad (47)$$

The frequency of the positive (RHP) zero is

$$\omega_{zp} = z_p = \frac{1}{LD}\left\{\frac{n-2D(n-1)}{[n-D(n-1)]}\right\} \times$$

$$\left\{\left[n(1-D)^2 R\left(1-\frac{V_F}{V_O}\right)+n(1-D)r\right]-Dr\right\}. \quad (48)$$

The LHP poles are

$$s_1, s_2 = -\omega_0\xi\left(1\pm\sqrt{1-\frac{1}{\xi^2}}\right) = -\omega_0\left(\xi\pm j\sqrt{1-\xi^2}\right). \quad (49)$$

The frequencies of the LHP poles are

$$f_{p1}, f_{p2} = f_0\xi\left(1\pm\sqrt{1-\frac{1}{\xi^2}}\right) = f_0\left(\xi\pm j\sqrt{1-\xi^2}\right). \quad (50)$$

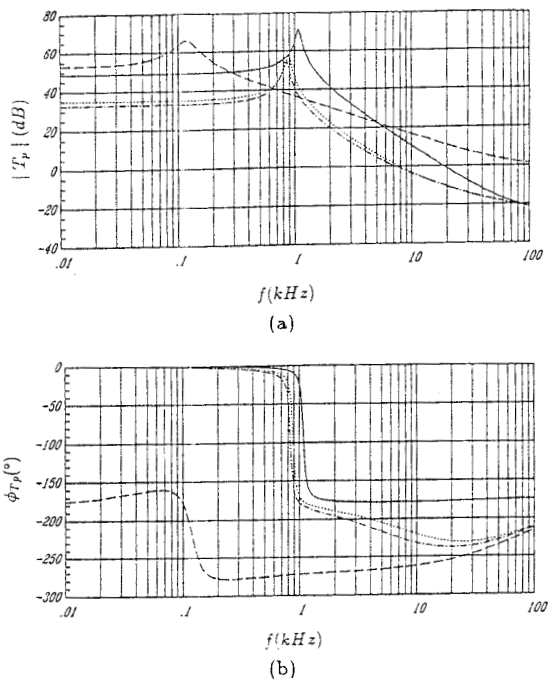

Fig. 9: Bode plots of T_p versus f for $D = 0.1$ (solid line), 0.35, 0.4, and 0.95. (a) $\mid T_p \mid$ versus f. (b) ϕ_{Tp} versus f.

The angular corner frequency is

$$\omega_0 = \sqrt{\frac{n^3(1-D)^2 R+[n-D(n-1)]r}{LC(R+r_C)[n-D(n-1)]}}. \quad (51)$$

The damping ratio is

$$\xi = \frac{\tau}{2\sqrt{\rho\times\gamma}} \quad (52)$$

where

$$\tau = n^3(1-D)^2 CRr_C+[Cr(R+r_C)+L][n-D(n-1)] \quad (53)$$

$$\rho = LC(R+r_C)[n-D(n-1)] \quad (54)$$

$$\gamma = n^3(1-D)^2 R+[n-D(n-1)]. \quad (55)$$

The Bode plot of the magnitude $\mid T_p \mid$ and the phase ϕ_{Tp} of the *control-to-output voltage transfer function* as functions of frequency f are shown in Figs. 9 (a) and (b) for V_O = 28 V, V_F = 0.7 V, C = 68 μF, L = 3 mH, r_C = 0.05 Ω, r_L = 1.7 Ω, r_{DS} = 0.5 Ω, R_F = 0.025 Ω, r_{T1} = 20 mΩ, r_{T2} = 10 mΩ, R = 95 Ω, turn ratio n = 5. and duty cycle D = 0.1 (solid line), 0.35, 0.40, and 0.95. It shows that the gain at low-frequencies is a constant. As the frequency increased up to 1 kHz, the gain started to falls with a slope of −40 dB/decade. The phase started at 0° and tends toward −180°. Since duty cycle increased beyond 0.6, the phase start to shift to −180°. The magnitude $\mid T_p \mid$ crosses 0 dB at 8 kHz for duty cycle D = 0.4. The phase shift decreases from 0° to −180° when duty cycle D approaches 1.

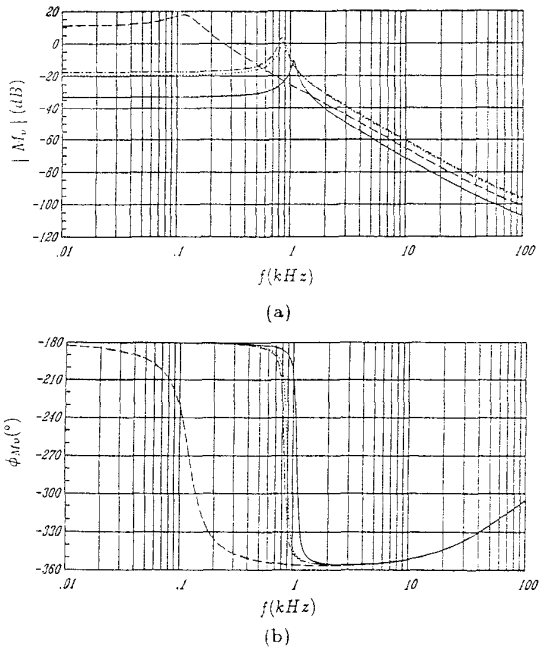

Fig. 10: Bode plots of M_v versus f for $D = 0.1$ (solid line), 0.35, 0.40, and 0.95. (a) $\mid M_v \mid$ versus f. (b) ϕ_{Mv} versus f.

B. Input-to-Output Voltage Transfer Function

The input-to-output voltage (or *line-to-output*) transfer function (or the *audio susceptibility*) was found using the small-signal model which is shown in Fig. 6. The result is

$$M_v(s) \equiv \frac{v_o(s)}{v_i(s)} \mid_{d(s)=0}$$

$$= -\frac{n^2 D(1-D)Rr_C}{L(R+r_C)[n-D(n-1)]} \frac{(s+\omega_{zn})}{s^2+2\xi\omega_o s+\omega_o^2}. \quad (56)$$

The plots of the magnitude $\mid M_v \mid$ and phase ϕ_{Mv} of the *input-to-output voltage transfer function* of flyback converter as functions of frequency f are shown in Figs. 10 (a) and (b) for $D = 0.1$ (solid line), 0.35, and 0.40, $R = 95\ \Omega$, $V_O = 28$ V, $V_F = 0.7$ V, $C = 68\ \mu$F, $L = 3$ mH, $r_L = 2\ \Omega$, $r_{DS} = 0.5\ \Omega$, $r_C = 0.05\ \Omega$, $n = 5$, and $R_F = 0.025\ \Omega$. At low frequencies, the magnitude of the input-to-output voltage transfer function $\mid M_v \mid$ increases as the duty cycle D increases, and the phase ϕ_{Mv} begins at $-180°$ at low frequencies.

C. Input Impedance

The open-loop input impedance of the flyback converter can be found using the small-signal model which is shown in Fig. 6. The final result is

$$Z_i(s) \equiv \frac{v_i(s)}{i_i(s)} \mid_{d(s)=0}$$

$$= \frac{[n-D(n-1)]L}{nD^2} \frac{s^2+2\xi\omega_0 s+\omega_o^2}{s+\omega_{rc}} \quad (57)$$

where

$$\omega_{rc} = \frac{1}{C(R+r_C)}. \quad (58)$$

The plots of the magnitude and phase of the *open-loop input impedance* of the flyback converter Z_i as a function of frequency f are shown in Figs. 11 for $D = 0.1$ (solid line), 0.35, 0.40, and 0.95, $R = 95\ \Omega$, $V_O = 28$ V, $V_F = 0.7$ V, $C = 68\ \mu$F, $L = 3$ mH, $r_L = 2\ \Omega$, $r_{DS} = 0.5\ \Omega$, $r_C = 0.05\ \Omega$, $r_{T1} = 20$ mΩ, $r_{T2} = 10$ mΩ, $n = 5$, and $R_F = 0.025\ \Omega$. At low frequencies, the magnitude of the open-loop input impedance $\mid Z_i \mid$ decreases as duty cycle D increases. The phase of this impedance starts at zero degrees and increases up to 90° at high frequencies.

D. Output Impedance

The open-loop output impedance of the flyback converter can be found using the small-signal model which is shown in Fig. 6. The result is

$$Z_o(s) \equiv \frac{v_t(s)}{i_t(s)} \mid_{d(s)=0 \text{ and } v_i(s)=0}$$

$$= \frac{Rr_C}{(R+r_C)} \frac{(s+\omega_{zn})(s+\omega_{ol})}{s^2+2\xi\omega_0 s+\omega_0^2} \quad (59)$$

where

$$\omega_{ol} = \frac{r}{L}. \quad (60)$$

The plots of the magnitude and phase of the *open-loop output impedance* of flyback converter as a function of frequency f are shown in Figs. 12 for $D = 0.1$ (solid line), 0.35, 0.40, 0.95, $R = 95\ \Omega$, $V_O = 28$ V, $V_F = 0.7$ V, $C = 68\ \mu$F, $L = 3$ mH, $r_L = 2\ \Omega$, $r_{DS} = 0.5\ \Omega$, $r_C = 0.05\ \Omega$, $r_{T1} =$

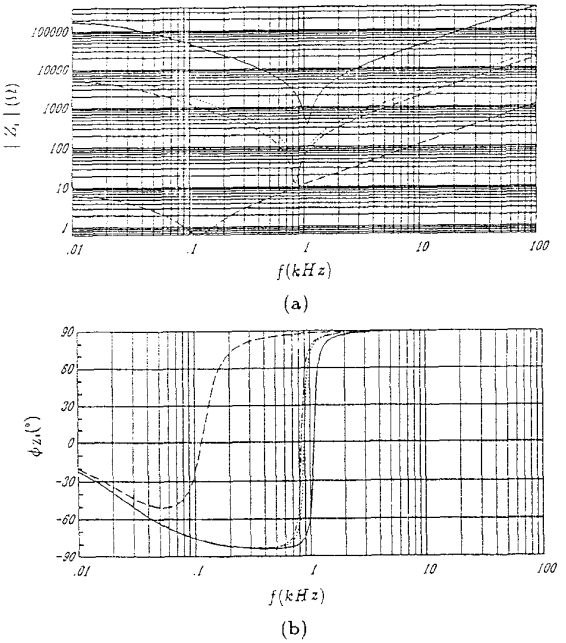

Fig. 11: Bode plots of Z_i versus f for $D = 0.1$ (solid line), 0.35, 0.4, and 0.95. (a) $\mid Z_i \mid$ versus f. (b) ϕ_{Zi} versus f.

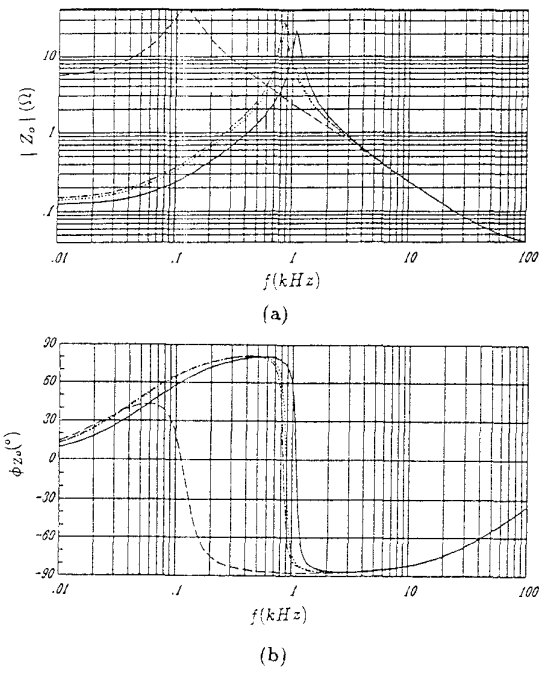

Fig. 12: Bode plots of Z_o versus f for $D = 0.1$ (solid line), 0.35, 0.4, and 0.95. (a) $\mid Z_o \mid$ versus f. (b) ϕ_{Zo} versus f.

20 mΩ, $r_{T2} = 10$ mΩ, $n = 5$, and $R_F = 0.025$ Ω. At low frequencies, the magnitude open-loop output impedance Z_o increases slightly as duty cycle D increases from 0 to 0.45. The phase of this impedance begins at zero degrees and decreases to $-90°$ at high frequencies.

VIII. Conclusions

A new method of modeling the PWM dc-dc switch-mode flyback converter operating in the continuous conduction mode for which the inductor current flows continuously has been presented. In this method, the static voltage and current transfer function for the idealized switching part of the converter are derived. The voltage and current sources for the dc and small-signal models are found from the steady-state analysis. The *principle of energy conservation* is used to determine an equivalent averaged resistances (EAR) of parasitic resistances. The proposed procedure leads to pure circuit models consisting of standard components. An important advantage of the models is that they can be used in circuit-simulation programs such as SPICE.

The effects of the duty cycle D on the dc and small-signal characteristics are illustrated. It is shown that the positive zero frequency of the control-to-output voltage transfer function of the converter moves from the right half of the s-plane to the left half of the s-plane as the duty cycle D approaches 1. In this case, the phase of the control-to-output voltage transfer function of the converter changes from 0° to $-180°$ at low frequencies. The Bode plots show that the gain $\mid T_p \mid$ of the control-to-output voltage transfer function of the converter is constant at low frequencies. As the frequency approaches 1 kHz, the gain starts to fall with a slope -40 dB/decade. The phase ϕ_{Tp} tends toward $-180°$ at high frequencies. The magnitude crosses zero at 8 kHz at the duty cycle $D = 0.45$. The positive zero frequency of the control-to-output voltage transfer function of the converter is zero when duty cycle D approaches 0.592578. Therefore, the duty cycle D greater than 0.6 is not recommended because of poor efficiency and poor dynamic response.

IX. Appendix

A power stage of PWM flyback dc-dc converter operating in continuous conduction mode shown in Fig. 1 will be designed to meet the following specifications: the input voltage is $V_I = 240$ to 300 VDC, $V_{I(norm)} = 270$ V, the output voltage is $V_O = 28$ VDC, the output current is $I_O = 0.2$ to 2 A, the operation switching frequency is $f_s = 100$ kHz, and the maximum allowable value of the peak-to-peak ripple voltage is $V_r/V_O \leq 1\%$.

The peak-to-peak ripple voltage is $V_r = 0.01 \times V_O = 0.01 \times 28 = 280$ mV. The minimum, nominal, and maximum values of the dc voltage transfer function are $M_{VDCmin} = V_O/V_{Imax} = 0.093$, $M_{VDCnom} = V_O/V_{Imin} = 0.1037$, $M_{VDCmax} = V_O/V_{Imin} = 0.117$, and Assuming the converter efficiency $\eta = 85\%$ and the maximum duty cycle $D_{max} = 0.37$, the transformer turns ratio is $n = \eta D_{max}/(1 - D_{max})M_{VDCmin} = (0.85 \times 0.37)/[(1 - 0.37) \times 0.093] \approx 5$. The corresponding values of the duty cycle are $D_{min} = nM_{VDCmin}/(nM_{VDCmin} + \eta) = (5 \times 0.093)/[(5 \times 0.093) + 0.85] = 0.35$, $D_{nom} = nM_{VDCnom}/(nM_{VDCnom} + \eta) = (5 \times 0.1037)/[(5 \times 0.1037) + 0.85] = 0.37$, and $D_{max} = nM_{VDCmax}/(nM_{VDCmax} + \eta) = (5 \times 0.117)/[(5 \times 0.117) + 0.85] = 0.40$. From the condition for continuous conduction mode, the minimum value of the inductor is

$$L_{min} = \frac{n^2 R_{max}(1 - D_{max})^2}{2 f_s}$$

$$= \frac{5 \times 5 \times 140 \times (1 - 0.40)^2}{2 \times 100 \times 10^3} = 7 \text{ mH}. \qquad (61)$$

The inductor was made using a Phillips ferrite pot core 3622 PA 275 3C8 and using 60 turns of Belden solid copper magnet wire with AWG 24. The measured inductance was $L = 7$ mH and the measured dc ESR of the inductor was $r_L = 1.7$ Ω.

The ESR of the tantalum filter capacitor of 68 μF measured at the switching frequency $f_s = 100$ kHz was $r_C = 33$ mΩ. The maximum value of the peak-to-peak voltage across the ESR is $V_{rC} = r_C I_{DMmax} = 0.33 \times 0.67 = 33.5$ mV. The maximum permissible value of the peak-to-peak voltage across the filter capacitor is $V_{Cmax} = V_r - V_{rC} = 280 - 33.5 = 0.246$ V. Therefore, the minimum capacitor is found as

$$C_{min} = \frac{I_{Omax} D_{max}}{f_s V_{Cmax}}$$

$$= \frac{2 \times 0.40}{100 \times 10^3 \times 0.246} = 32.45 \ \mu\text{F}. \qquad (62)$$

The standard value of 68 μF was chosen as the filter capacitance. The switching components used were an International Rectifier power MOSFET IRF 620 (200V/9A) with the ON–resistance $r_{DS} = 0.4\ \Omega$ and Motorola power diode MUR 820 (200V/8A) with forward resistance $R_F = 0.02\ \Omega$ and $V_F = 0.7$ V.

REFERENCES

[1] R. D. Middlebrook and S. Ćuk, *Advances in Switched–Mode Power Conversion.* vols. I and II. Pasadena, CA: TESLAco, 1981.

[2] R. D. Middlebrook and S. Ćuk, "A general unified approach to modeling switching–converter power stages," *IEEE Power Electronics Specialists Conference Record*, 1976, pp. 18–34.

[3] W. M. Polivka, P. R. K. Chetty, and R. D. Middlebrook, "State–space average modeling of converters with parasitics and storage time modulation," *IEEE Power Electronics Specialists Conference Record*, 1980, pp. 119–143.

[4] R. P. Severns and G. Bloom, *Modern DC–to–DC Switch–mode Power Converter Circuits.* New York: Van Nostrand, 1985, pp. 30–42 and 130–135.

[5] Y. S. Lee, "A systematic and unified approach to modeling switches in switch–mode power supplies," *IEEE Trans. Ind. Electron.*, vol. IE–32, pp. 445–448, Nov. 1985.

[6] V. Vorpérian, "Simplified analysis of PWM converters using the PWM switch, Part I: Continuous conduction mode," *IEEE Trans. Aerospace and Electronic Systems*, vol. AES–26, pp. 497–505, May 1990.

[7] D. Czarkowski and M. K. Kazimierczuk, "Static– and dynamic–circuit models of PWM buck–derived DC–DC converters," *IEE Proc. Pt. G, Circuits, Devices and Systems*, vol. 139, no. 6, pp. 669–679, Dec. 1992.

[8] D. Czarkowski and M. K. Kazimierczuk, "SPICE compatible averaged models of PWM full–bridge dc–dc converter," pp. 669–679, *Proceedings of 1992 International Conference on Industrial Electronics, Control, and Instrumentation (IECON'92)*, 1992, vol. 1, pp. 488–493.